

# Surface Activity of Lysozyme and Dipalmitoyl Phosphatidylcholine Vesicles at Compressed and Supercritical Fluid Interfaces

Geoffrey D. Bothun,<sup>†</sup> Yeh Wei Kho,<sup>‡</sup> Jason A. Berberich,<sup>‡</sup> Justin P. Shofner,<sup>‡</sup> Tracy Robertson,<sup>‡</sup> Kevin J. Tatum,<sup>‡</sup> and Barbara L. Knutson<sup>\*‡</sup>

NSF–STC Environmentally Responsible Solvents and Processes, Department of Mechanical and Chemical Engineering, North Carolina A&T State University, Greensboro, North Carolina 27411, Department of Chemical and Materials Engineering, University of Kentucky, Lexington, Kentucky 40506

Received: August 29, 2005; In Final Form: October 31, 2005

The surface activities of lysozyme and dipalmitoyl phosphatidylcholine (DPPC) vesicles at aqueous/compressed fluid interfaces are examined via high-pressure interfacial tension measurements using the pendant drop technique. The density and interfacial tension in compressible fluid systems vary significantly with pressure, providing a versatile medium for elucidating interactions between biomolecules and fluid interfaces and a method to elicit pressure-dependent interfacial morphological responses. The effects of lysozyme concentration (0.0008, 0.01, and 1 mg/mL) and pressure ( $\geq 7$  MPa) on the dynamic surface response in the presence of ethane, propane, N<sub>2</sub>, and CO<sub>2</sub> at 298 K were examined. Interfacial lysozyme adsorption reduced the induction phase and quickly led to interfacial tensions consistent with protein conformational changes and monolayer saturation at the compressed fluid interfaces. Protein adsorption, as indicated by surface pressure, correlated with calculated Hamaker constants for the compressed gases, denoting the importance of dispersion interactions. For DPPC at aqueous/compressed or aqueous/supercritical CO<sub>2</sub> interfaces (1.8–20.7 MPa, 308 K), 2–3-fold reductions in interfacial tension were observed relative to the pure binary fluid system. The resulting surface pressures infer pressure-dependent morphological changes within the DPPC monolayer.

## Introduction

Interactions between biomolecules and fluid interfaces can dictate the biocompatibility and recovered biocatalyst activity in a variety enzymatic and whole-cell bioprocesses including biphasic biosynthesis, bioseparations, and product formulation.<sup>1,2</sup> Amphiphilic biomolecules, such as proteins and cellular membrane components (and their self-assemblies), are surface-active; the rate and extent of their interfacial adsorption is dependent on the properties of the nonaqueous fluid phase. However, unlike traditional surfactants, proteins are capable of significant conformational rearrangement after interfacial adsorption. These changes in conformation further reduce the interfacial tension, resulting in dynamic protein adsorption behavior<sup>3</sup> and potential protein denaturation.

Lipid vesicles (liposomes) can be employed as model cell membranes to investigate membrane stability and whole-cell catalytic activity at aqueous/fluid interfaces. Similar to protein denaturation, interfacial destabilization of vesicles is a dynamic event that is governed by the nature of the fluid interface. Vesicle adsorption is followed by a disruption of the bilayer(s) and the formation of a lipid monolayer.<sup>4</sup> Pseudo-equilibrium is then established, in which vesicles in the bulk aqueous phase continue to adsorb and are exchanged with vesicles that form by lipid desorption from the interfacial monolayer. This phenomenon has been used to form unilamellar liposomes in water/liquid alkane systems.<sup>5</sup> The extent of interfacial destabilization influences liposome formation, stability, and the activity

of membrane-bound components, such as proteins. In addition to the nature of the aqueous/fluid interface, physicochemical protein and vesicle properties such as size and surface charge can influence conformation and stability, respectively.

Investigation of the surface activity of biomolecules is motivated by recent advances in compressed and supercritical fluid technologies. Compressed and supercritical fluids are increasingly used as alternative solvents for bioprocessing based on their pressure-tunable solvent strength and the ability to recover a solvent-free product following system depressurization.<sup>6,7</sup> Compressed or supercritical CO<sub>2</sub> ( $T_c = 304$  K,  $P_c = 7.4$  MPa) offers the additional benefits of being nonflammable, nontoxic, inexpensive, and suitable for the processing of thermally labile compounds, such as pharmaceuticals. Successful applications of compressed solvents in bioprocesses include enzymatic and whole-cell biocatalysis,<sup>8–12</sup> inverse emulsion protein extraction,<sup>13</sup> and antisolvent precipitation of proteins.<sup>14</sup> Emerging applications of CO<sub>2</sub>-based technologies include liposome formation and processing<sup>15,16</sup> and the microbial sterilization of bulk aqueous phases<sup>17</sup> and biodegradable polymeric matrixes.<sup>18</sup> Examining biomolecule adsorption at compressed and supercritical fluid interfaces is relevant to optimizing the activity and yields of recovered proteins, controlling the morphology and encapsulation efficiency of liposomes, and investigating whole-cell inactivation.

Compressed and supercritical fluid technologies also provide a versatile medium for elucidating interactions between biomolecules and fluid interfaces. The pressure-tunable physicochemical properties of the fluid and the aqueous/pure fluid interfacial tension greatly impact the affinity of biomolecules for the fluid and subsequent interfacial adsorption. This concept has been demonstrated for a broad range of CO<sub>2</sub>-philic surfac-

\* Author to whom correspondence should be addressed. E-mail: bknutson@engr.uky.edu.

<sup>†</sup> North Carolina A&T State University.

<sup>‡</sup> University of Kentucky.

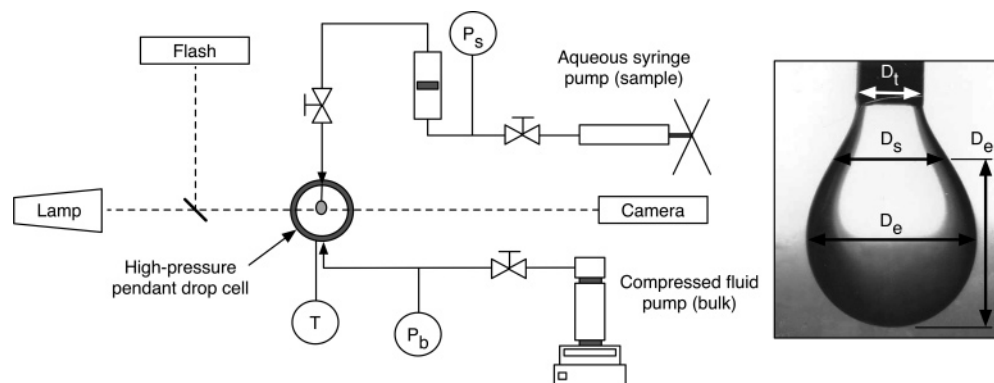


**Figure 1.** High-pressure pendant drop interfacial tensiometer and a representative photograph of a magnified aqueous pendant drop in  $N_2$  at 7.0 MPa and 298 K with the characteristic drop dimensions used for analysis (defined in text). T represents the temperature probe and  $P_s$  and  $P_b$  represent the pressure gauges for the sample and bulk phases, respectively.

tants, for which the equilibrium interfacial tension has provided significant understanding of solvation and aggregation (see Shah et al.<sup>19</sup> for a review). The surface activity of biomolecules may be manipulated using a single compressed or supercritical fluid by varying pressure, providing a way to potentially stabilize emulsions in compressed and supercritical fluids using biological surface-active agents. Previous investigations of protein adsorption at compressed and supercritical fluid interfaces have focused on ovalbumin at gaseous and supercritical  $CO_2$ /water interfaces.<sup>20</sup>

This study examines the surface activity of lysozyme and dipalmitoyl phosphatidylcholine (DPPC) vesicles at aqueous interfaces in the presence of compressed and supercritical fluids. Lysozyme, a 14.3 kDa globular protein with an isoelectric point of approximately pH 11, was chosen as a model enzyme due to its well-characterized structure and function. DPPC is a 734 Da zwitterionic phospholipid with dual  $C_{16}$  alkane tails and a choline headgroup. DPPC is also an abundant and well-characterized biological phospholipid. The bilayer vesicles formed by DPPC are frequently used as model cellular membranes. Interfacial tension is determined as a function of time and pressure (i.e., fluid density or solvent strength) using a high-pressure pendant drop apparatus. The time-dependent and pseudo-equilibrium adsorption behavior of lysozyme and DPPC vesicles is interpreted in terms of the interaction potential due to van der Waals forces, as described by the pure fluid and effective Hamaker constants.

## Experimental Methods

**Materials.** Nitrogen (ultrahigh purity), carbon dioxide (zero grade), and ethane (chemically pure grade) were obtained from Scott Gross Company. Propane (high purity) was purchased from MG Industries (Malvern, PA). Chicken egg white lysozyme (salt-free, albumin-free) was obtained from ICN Biomedicals Inc. and used as received. Enzyme solutions were prepared using a 0.05 M sodium phosphate buffer solution with initial solution pH adjusted to 7.0. Dipalmitoyl phosphatidylcholine (DPPC) was purchased from Sigma. Multilamellar vesicles were prepared as previously described<sup>21</sup> with 0.1 mM DPPC in deionized ultrafiltered water (100–200 nm in diameter based on dynamic light scattering, data not shown). All other reagents were obtained from commercial sources.

**Interfacial Tension Measurements.** The high-pressure pendant drop apparatus (Figure 1) was designed and constructed by DB Robinson Research Ltd. (Edmonton, Canada). It consists of a 15 mL stainless steel view cell with sapphire windows, an observation lamp, flash, microscope, and a Polaroid camera.

The view cell and sample cylinders are housed in a stainless steel temperature-controlled box. The box, flash, observation lamp, and beam splitter are mounted on a vibration-free table. In this work, the aqueous solution and compressed or supercritical fluid were supplied by a manual syringe pump (High-Pressure Equipment Company, Erie, PA) and an automated ISCO syringe pump (Lincoln, NB), respectively. A small stainless steel needle of known diameter ( $D_t$ ) protruding from the top of the view cell was used to form the aqueous solution pendant drop in the bulk phase of the compressed or supercritical fluid (Figure 1). Before a droplet was formed, the aqueous phase was presaturated with the fluid at temperature and pressure. A short stabilization period was required ( $<1$  min) between initial droplet formation and measurement, where the first measurement corresponded to  $t = 0$ .

The dynamic interfacial tension behaviors of protein and DPPC vesicle solutions were determined from photographs of the droplet as a function of time. The method of the selected plane, an empirical evaluation of the Laplace equation, was used to calculate the interfacial tension from the drop shape (as described by Ambwani and Fort<sup>22</sup>)

$$\gamma = \Delta\rho g D_e^2 (1/H) \quad (1)$$

where  $\gamma$  is the interfacial tension,  $\Delta\rho$  is the density difference between the fluids in contact,  $g$  is the gravity constant, and  $D_e$  is the drop diameter at the equatorial plane. The correction factor  $1/H$ , which relates the pendant drop shape to that of a sphere, was determined from the drop profile  $D_s/D_e$ , as tabulated by Stauffer.<sup>23</sup>  $D_s$  is the diameter at the plane a distance of  $D_e$  from the tip of the pendant drop (Figure 1). The interfacial tensions of the  $N_2$ /water system as a function of pressure were within 5% of literature values.<sup>24</sup>

## Results and Discussion

**Surface Activity of Lysozyme at Compressed Fluid Interfaces.** The surface activity of lysozyme at a compressed fluid/water interface is reported in terms of dynamic surface pressure  $\Pi(t)$ , which is the difference between the equilibrium interfacial tension  $\gamma_0$  at the pure compressed fluid/water interface and the dynamic interfacial tension  $\gamma(t)$  of the aqueous solution containing the surface-active agent at the identical temperature and pressure

$$\Pi(t) = \gamma_0 - \gamma(t) \quad (2)$$

The variable  $t$  is the elapsed time of the stabilized droplet, where

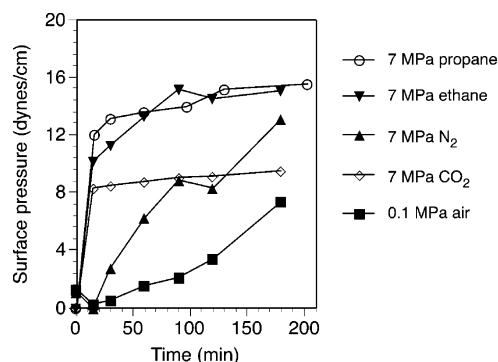


**Figure 2.** Dynamic surface pressure response of lysozyme (0.01 mg/mL in aqueous phase) at 298 K in the presence of different compressed fluids at 7.0 MPa. Results are compared to air at 0.1 MPa.

$t = 0$  denotes the first interfacial tension measurement. Thus, the surface pressure may be nonzero at  $t = 0$  because it is calculated relative to the equilibrium value at the pure  $\text{CO}_2$ /water interface. Positive surface pressures indicate that the surface-active agent adsorbs at an interface.

Protein adsorption at weak solvent interfaces, such as air, is characterized by an induction period (regime I), in which the protein diffuses to the interface and a small reduction in interfacial tension, or small increase in surface pressure, is observed.<sup>3,25</sup> The induction period is followed by a dynamic decrease in interfacial tension as the protein adsorbs to the interface and changes conformation (regime II). Finally, the interface becomes saturated with protein, and a multilayer “gel” may form at high protein concentrations (regime III). Given the extensive tertiary structure in proteins, a substantial time period may be required to reach a constant interfacial tension, where the existence of a true equilibrium is controversial.<sup>3</sup> Therefore, the extent of interfacial tension reduction is customarily described as an apparent, or pseudo-equilibrium, interfacial tension taken at a predetermined time or calculated via data extrapolation.

**Effect of Compressed Fluid Phase on Lysozyme Surface Activity.** In aqueous lysozyme solutions the rate and magnitude of the dynamic surface pressure response is dependent on the nature of the compressible fluid (Figure 2). At 7.0 MPa, rapid lysozyme adsorption occurs at the propane, ethane, and  $\text{CO}_2$  interface, relative to air at 0.1 MPa, with no observable induction time ( $<15$  min). This observation suggests appreciable lysozyme adsorption followed by significant conformational changes in the protein (regime II). Lysozyme adsorption at the propane and  $\text{CO}_2$  interface at 7.0 MPa appears to enter regime III (monolayer saturation) after 15 min of exposure to the interface, more rapidly than in the presence of ethane. Ethane and propane are liquids at the experimental conditions and exhibit the greatest increase in surface pressure, consistent with more “oil-like” interfaces. At strongly adsorbing interfaces, our pendant drop technique cannot capture the rapid changes in interfacial tension associated with short induction periods. Similarly, Beverung et al.<sup>3</sup> were unable to quantify the induction period for proteins at oil/water interfaces, where the behavior quickly proceeds to regime III.

Nitrogen has a much lower reduced density ( $\rho_r = \rho/\rho_c$ ) at 7.0 MPa and 298 K relative to ethane and propane ( $\text{N}_2$ , 0.25; ethane, 1.76; and propane, 2.31), indicating a lower solvent strength. Hence, an apparent induction time is observed in the presence of pressurized  $\text{N}_2$ , which is followed by a slower rate of protein adsorption and conformational changes at times  $>15$  min. In contrast, a distinct induction time of 60 min is observed

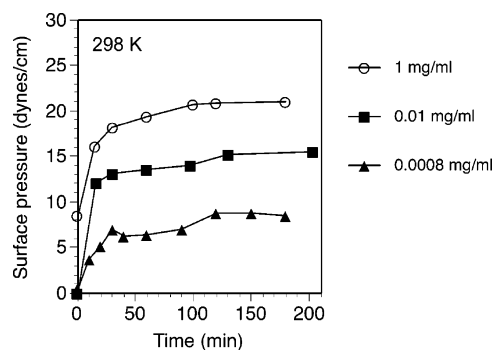


**Figure 3.** Dynamic surface pressure response of lysozyme at the propane/water interface at 7.0 MPa and 298 K as a function of aqueous protein concentration.

in the presence of air at 0.1 MPa, which has minimal solvent strength. Monolayer saturation is not apparent for air or  $\text{N}_2$ . Increased surface activity of proteins at the oil/water interface relative to the air/water interface has been observed previously for the water/liquid hydrocarbon systems.<sup>3,26</sup> Unlike the air/water interfaces, the hydrophobic portions of proteins adsorbing at oil/water interfaces can penetrate into the oil phase.<sup>26</sup> In addition, oil/water interfaces generally exhibit a negative surface potential due to preferential binding of anions.<sup>27</sup> The isoelectric point of lysozyme is  $\text{pH} \sim 11$ ; therefore, the protein exhibits a net positive surface charge at  $\text{pH} 7$ . At small separations, attractive electrostatic double-layer forces between positively charged lysozyme and negatively charged oil + anion interfaces increase lysozyme adsorption relative to air.<sup>28</sup> We have found no information concerning anion binding at compressed  $\text{CO}_2$  interfaces.

**Effect of Lysozyme Concentration at the Propane/Water Interface.** Below the conditions for monolayer saturation (for a given interface) the rate of protein adsorption and dynamic surface pressure response is dependent on the aqueous protein concentration. The dynamic adsorption behavior for varying lysozyme concentrations at the aqueous/compressed propane interface is typical of protein adsorption at oil/water interfaces (Figure 3). Increasing the lysozyme concentration leads to a greater rate of lysozyme adsorption and a greater apparent equilibrium surface pressure. An induction period is not observed at any of the aqueous lysozyme concentrations measured (0.0008, 0.01, or 1.0 mg/mL). At 1 mg/mL lysozyme initial protein adsorption could not be captured due to the time scale measurable by the pendant drop technique. Protein diffusion to the interface increases with bulk phase concentration, leading to rapid interfacial adsorption occurring on a short time scale.

The rate of lysozyme adsorption at the aqueous/compressed  $\text{N}_2$  interface increases with increasing protein concentration (data not shown), similar to that observed for propane. An increase in lysozyme concentration from 0.01 to 1 mg/mL increases the driving force for adsorption (via diffusion) at the  $\text{N}_2$  interface and reduces the induction period, as observed in Figure 2 for 0.01 mg/mL. The dynamic surface pressure response and apparent equilibrium surface pressure at 1 mg/mL lysozyme are similar for  $\text{N}_2$  and propane at 7.0 MPa.

**Effect of Propane and  $\text{CO}_2$  Solvent Strength on Lysozyme Surface Activity.** Perhaps the greatest utility of compressed and supercritical fluids is the ability to manipulate density, or solvent strength, using pressure and temperature. Changes in fluid density alter attractive interactions between the proteins and the aqueous/fluid interface. The initial rate of lysozyme adsorption



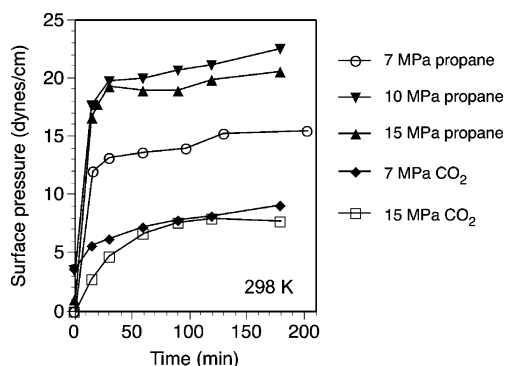


**Figure 4.** Dynamic surface pressure response of lysozyme (0.01 mg/mL aqueous concentration) at the aqueous/compressed fluid interface as a function of CO<sub>2</sub> or propane pressure at 298 K.

at the aqueous/propane and aqueous/CO<sub>2</sub> interfaces is sensitive to system pressure (Figure 4). In the case of propane, an increase in the initial rate of adsorption and the pseudo-equilibrium surface pressure is observed as the pressure is increased from 7 to 10 MPa. However, the rates of adsorption at 10.0 and 15.0 MPa are indistinguishable given the uncertainty of the time-dependent surface pressure measurements ( $\pm 5\%$ ), which is based on multiple experiments and intrinsic equipment error. In contrast, increasing pressure reduces the initial rate of lysozyme adsorption at the aqueous/CO<sub>2</sub> interface (Figure 4). Minimal variation in the dynamic behavior of lysozyme adsorption (0.01 mg/mL) at the aqueous/N<sub>2</sub> interface was observed at 298 K and pressures of 0.1, 3.5, and 7.0 MPa (data not shown), consistent with the low solvent power of N<sub>2</sub>.

Several factors may contribute to the reduced surface pressure of lysozyme in the presence of CO<sub>2</sub> relative to the hydrocarbon systems. First, the solvation of lysozyme in CO<sub>2</sub> and CO<sub>2</sub>-saturated water is expected to be different than in corresponding hydrocarbon solutions. CO<sub>2</sub> ( $\rho_r = 1.59$ ) has a reduced density at 298 K and 7.0 MPa than ethane (1.76) or propane (2.31), which suggests a reduced solvating power. Compressed CO<sub>2</sub> is neither hydrophilic nor hydrophobic,<sup>29</sup> further suggesting poor solvation of the hydrophobic regions of the surface-active protein relative to ethane and propane. In addition, the solvation of lysozyme in the CO<sub>2</sub> phase will be affected by the solubility of water in this phase as well as the potential of CO<sub>2</sub> to participate in Lewis acid interactions with the biomolecule.<sup>30</sup> Second, the interfacial tension of CO<sub>2</sub>/water (35.1 dynes/cm) is lower than that of propane (46 dynes/cm), ethane (38.1 dynes/cm), or N<sub>2</sub> (68.4 dynes/cm) at 298 K and 7.0 MPa and air (72 dynes/cm) at 298 K and 0.1 MPa. Thus, a lower dynamic interfacial tension is required to achieve an equivalent surface pressure (eq 2) at the CO<sub>2</sub>/water interface relative to the other compressed solvents. Third, the buffering solution (0.05 M sodium phosphate) is not adequate to counteract the effect of carbonic acid formation by the dissolved carbon dioxide in water ( $\text{CO}_2 + \text{H}_2\text{O} \rightleftharpoons \text{H}_2\text{CO}_3 \rightleftharpoons \text{H}^+ + \text{HCO}_3^- \rightleftharpoons 2\text{H}^+ + \text{CO}_3^{2-}$ ). At 295 K the dissolution of compressed CO<sub>2</sub> (3.5–13.9 MPa) in a 0.05 mM phosphate buffer solution yielded a calculated pH of 4.9.<sup>21</sup> Lowering the pH will increase the positive charge on lysozyme, relative to the hydrocarbon, air, and N<sub>2</sub> systems (constant at pH 7) and alter the electrostatic double-layer interactions between the lysozyme and the CO<sub>2</sub> interface. If the CO<sub>2</sub> interface is neutral, then an increase in positive protein charge will enhance repulsion. In contrast, if anions bind to liquid CO<sub>2</sub>/water interfaces similar to oil/water interfaces, then this increase in charge will enhance attraction at short separations.

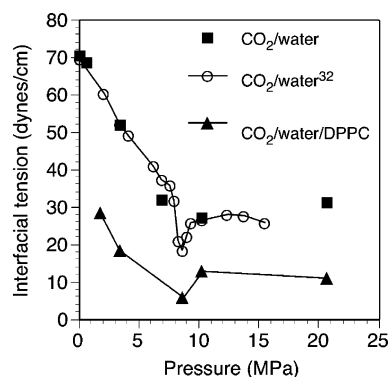


**Figure 5.** Pseudo-equilibrium interfacial tension ( $> 15$  min) of DPPC relative to the pure CO<sub>2</sub>/water interface as a function of pressure at 308 K. DPPC was present as multilamellar vesicles in the aqueous phase (0.1 mM). CO<sub>2</sub>/water interfacial tensions are compared to those from Chun and Wilkinson.<sup>32</sup>

Finally, Tewes and Boury<sup>31</sup> recently demonstrated the interplay between the adsorption of ovalbumin (OVA, 42 kDa globular protein) and the formation of CO<sub>2</sub>/water clusters at the CO<sub>2</sub>/water interface. Between 0.0229 and 0.523 mg OVA/mL, adsorption was not influenced by the formation of a CO<sub>2</sub>–H<sub>2</sub>O cluster network until 9.0 MPa, at which point a new interfacial protein–H<sub>2</sub>O–CO<sub>2</sub> complex was suspected and a lower surface pressure was observed relative to the 5.0–8.0 MPa region. Comparatively, we observed a significantly lower initial rate of lysozyme adsorption and slightly lower pseudo-equilibrium surface pressure at 15.0 MPa than at 7.0 MPa. This occurred at a lower protein concentration (0.01 mg/mL) than observed for OVA; however, lysozyme (14.3 kDa) is smaller than OVA (42 kDa), which may permit more penetration into the cluster interphase.<sup>20</sup> An increase in cluster organization at 15.0 MPa and a potential lysozyme–H<sub>2</sub>O–CO<sub>2</sub> complex may have reduced lysozyme adsorption and interphase penetration relative to 7.0 MPa, producing a lower surface pressure.

**Destabilization of DPPC Vesicles at the Compressed CO<sub>2</sub> Interface.** A reduction in the dynamic interfacial tension relative to the pure CO<sub>2</sub>/water interface demonstrates that DPPC vesicles rapidly adsorb ( $< 15$  min) and disintegrate at the compressed and supercritical CO<sub>2</sub> interface (equilibrium values shown in Figure 5). Vesicle disintegration includes the adsorption of vesicles at the interface followed by bilayer disruption into monolayers.<sup>4</sup> With the exception of 8.7 MPa, increasing pressure from 1.8 to 20.7 MPa leads to a reduction in interfacial tension with increased CO<sub>2</sub> solvent strength (density). The low interfacial tension measured at 8.7 MPa is consistent with a minimum in the interfacial tension of a pure aqueous/compressed CO<sub>2</sub> system of 8.62 MPa at 308 K (Figure 5).<sup>32</sup> This minimum, observed by multiple investigators, may also be an artifact of temperature gradients in the experimental apparatus, which lead to inaccuracies in the corresponding densities near the vapor–liquid or vapor–supercritical transition.<sup>33</sup>

Trends in DPPC surface activity are dependent on the morphology of both the bilayer vesicles and the insoluble monolayer. Previous investigations have demonstrated the relationship between the main phase transition, or melting temperature ( $T_m$ ), of aqueous bilayer vesicles and the extent and rate of monolayer adsorption at the air/water interface.<sup>34,35</sup> Below  $T_m$ , the monolayer is gellike and referred to as a liquid-condensed (LC) phase. As the temperature increases, a transition to a fluidlike bilayer is observed at  $T_m$  in both intact vesicles and monolayers adsorbed at the air–water interface, resulting

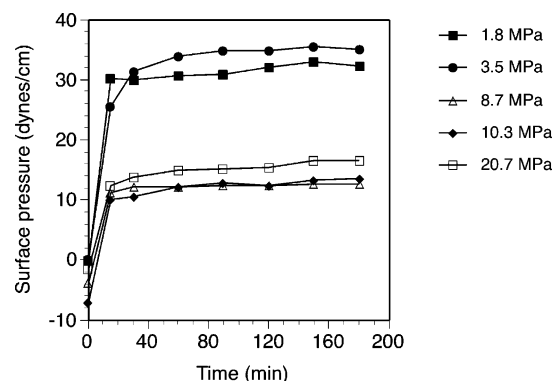


**Figure 6.** Dynamic surface pressure of DPPC at the aqueous/compressed CO<sub>2</sub> interface as a function of pressure at 308 K. DPPC was present as multilamellar vesicles in the aqueous phase (0.1 mM).

in an increase in surface pressure. This fluidlike monolayer is referred to as a liquid-expanded (LE) phase.

We have recently demonstrated CO<sub>2</sub>-induced gel-to-fluid phase transitions in aqueous liposome solutions using fluorescence anisotropy.<sup>21</sup> The main phase transition temperature of DPPC vesicles was reduced from 315 K at atmospheric pressure (no CO<sub>2</sub> present) to 310 and 299 K in the presence of CO<sub>2</sub> at 1.8 and 7.0 MPa, respectively. The phase transition was also broadened, spanning from 307 to 311 K (1.8 MPa CO<sub>2</sub>) and 295 to 301 K (7.0 MPa CO<sub>2</sub>). The reduction in melting temperature was attributed to the accumulation of CO<sub>2</sub> within the bilayer due to high aqueous CO<sub>2</sub> concentrations under elevated pressures. Reductions in pH due to carbonic acid formation did not alter the main phase transition, consistent with previous works that show DPPC melting is unaffected above pH 3 due to the low pK<sub>a</sub> (~2–3) of the phosphate moiety in the DPPC headgroup.<sup>36</sup> Therefore, we do not expect carbonic acid formation to significantly alter the morphology of interfacial DPPC monolayers.

Two distinct regions of DPPC surface pressure are observed at high (≥8.7 MPa) and low (1.8 and 3.5 MPa) CO<sub>2</sub> pressures (Figure 6). At pressures ≥8.7 MPa, the surface pressure response due to DPPC adsorption is clearly not a strong function of CO<sub>2</sub> pressures at 308 K. Our previous observation that bulk DPPC vesicles are in a fluidlike phase at these conditions<sup>21</sup> suggests that these surface pressures correspond to a more loosely packed LE DPPC monolayer at the CO<sub>2</sub>/water interface. However, at 1.8 MPa and 308 K the bilayer exists within the phase transition region and contains both gel and fluid domains. Furthermore, interpolating our previous results<sup>21</sup> suggests that the DPPC phase transition at 308 K occurs near 3.3 MPa CO<sub>2</sub>. Therefore, DPPC monolayers contain coexisting LE and LC domains at 1.8 and 3.5 MPa CO<sub>2</sub>. In mixed LE–LC monolayers, the LC domains repel one another to yield an ordered monolayer structure. For instance, Li et al.<sup>37</sup> showed that DPPC forms ordered LE–LC monolayers at the chloroform/water and dodecane/water interfaces below *T<sub>m</sub>*.

The surface pressure trends are not identical to those observed at the air/water interface for dimyristoyl phosphatidylcholine (DMPC, dual C<sub>14</sub> tails, and a choline headgroup), which exhibits a lower surface pressure in the liquid-condensed phase (gel-like) than the liquid-expanded phase (fluid-like).<sup>34</sup> In this case, a high interfacial tension is observed at the pure air/water interface ( $\gamma_o = 72$  dynes/cm) at 298 K, which is close to the DMPC melting temperature (*T<sub>m</sub>* ≈ 296 K).<sup>36</sup> The low surface tensions in LE DMPC monolayers (above the phase transition) yield higher surface pressure values ( $\Pi(t) = \gamma_o - \gamma(t)$ ).

**TABLE 1: Pseudo-Equilibrium Interfacial Tensions and Calculated Effective Hamaker Constants (*A*<sub>132</sub>) at 298 K for Aqueous Lysozyme (0.01 mg/mL) at Compressed Fluid Interfaces and the Air Interface**

	pressure (MPa)	IFT <sup>a</sup> (dynes/cm)	Hamaker constant ( <i>A</i> <sub>132</sub> , 10 <sup>−22</sup> J) <sup>b</sup>
ethane	7.0	21.3	−5.6
propane	7.0	29.8	0.9
	10.0	23.1	1.2
N <sub>2</sub>	7.0	49.4	−15.1
CO <sub>2</sub>	7.0	26.0	−9.9
	15.0	18.6	−9.0
air	0.1	61.6	−16.0

<sup>a</sup> Pseudo-equilibrium interfacial tension (time > 180 min). <sup>b</sup> On the basis of *A*<sub>22</sub> = 4.0 × 10<sup>−20</sup> J (calculated from lysozyme at air/water interface using eq 4)<sup>28</sup> and *A*<sub>33</sub> = 3.7 × 10<sup>−20</sup> (water).<sup>39</sup>

**TABLE 2: Pseudo-Equilibrium Interfacial Tensions and Calculated Effective Hamaker constants (*A*<sub>132</sub>) for Aqueous DPPC at Compressed and Supercritical CO<sub>2</sub> Interfaces (308 K) and the Air Interface (308 and 318 K)<sup>34</sup>**

	pressure (MPa)	IFT <sup>a</sup> (dynes/cm)	Hamaker constant ( <i>A</i> <sub>132</sub> , 10 <sup>−22</sup> J) <sup>b</sup>
CO <sub>2</sub>	1.8	28.5	−166.8
	8.7	5.4	−149.0
	20.7	11.1	−99.4
air	0.1	59 (308 K) <sup>c</sup> 39 (318 K) <sup>d</sup>	−171.0

<sup>a</sup> Pseudo-equilibrium interfacial tension (IFT; time = 180 min). <sup>b</sup> On the basis of *A*<sub>22</sub> = 7.9 × 10<sup>−20</sup> J (DPPC, calculated from lipid–water–lipid interaction using eq 4)<sup>42</sup> and *A*<sub>33</sub> = 3.7 × 10<sup>−20</sup> (water).<sup>39</sup> <sup>c</sup> IFT with gel phase (0.56 mM DPPC and 1 mM NaCl).<sup>34</sup> <sup>d</sup> IFT with fluid phase (0.56 mM DPPC and 1 mM NaCl).<sup>34</sup>

Comparatively, we also observe lower interfacial tensions in DPPC monolayers at the CO<sub>2</sub>/water interface with increasing pressure (Figure 6). However, the pure CO<sub>2</sub> water interfacial tension ( $\gamma_o$ ) is decreasing simultaneously, leading to our unique observation that LE monolayers result in lower surface pressures than LC monolayers at this CO<sub>2</sub>/water interface.

The initial negative values of some DPPC surface pressures suggests that, despite the presaturation of the aqueous phase with CO<sub>2</sub>, the interface is not fully developed at *t* = 0 (Figure 6). However, with the exception of 3.5 MPa, a pseudo-equilibrium is reached at 15 min due to DPPC adsorption at compressed and supercritical CO<sub>2</sub> interfaces. In contrast, Panaiotov et al.<sup>35</sup> have shown that the dynamic surface pressure response due to DMPC adsorption at the air/water interface does not equilibrate within 60 min with high spreading volumes at 298 K. Low surface pressures (high interfacial tensions) observed for DPPC at the air/water interface (Table 2)<sup>34</sup> also suggest that interfacial adsorption is significantly lower than at the CO<sub>2</sub> interface. In fact, DPPC surface pressures at 1.8 and 3.5 MPa CO<sub>2</sub> pressure and 308 K closely resemble that of the chloroform/water interface at 295 K.<sup>37</sup> Liposome spreading at compressed and supercritical CO<sub>2</sub> interfaces may be used to form monolayer films much quicker than an N<sub>2</sub>/water (or air/water) system at atmospheric pressure without introducing potentially hazardous or toxic organic solvents.

**Dispersion Interactions at Compressed Fluid Interfaces.** Colloidal theory provides a qualitative description of the observed dynamic adsorption behavior of biomolecules. Dispersion forces play a primary role in the initial adsorption processes of proteins<sup>28</sup> and phosphatidylcholine vesicles<sup>38</sup> at oil/water and air/water interfaces. The dispersion interactions between macroscopic bodies can be described using the Hamaker–de Boer approximation.<sup>39</sup> For a sphere interacting with a planar surface

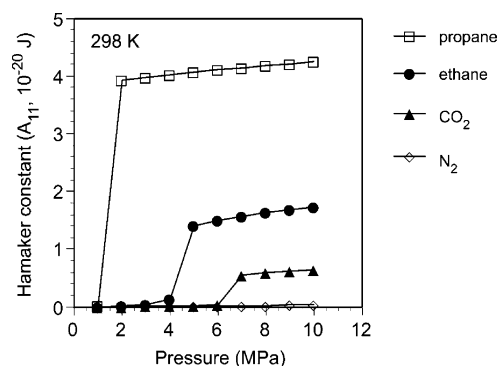


**Figure 7.** Calculated pure fluid Hamaker constant ( $A_{11}$ ) for propane, ethane, CO<sub>2</sub>, and N<sub>2</sub> as a function of pressure at 298 K.

the contribution from the van der Waals (vdW) interaction to the Gibbs energy of adsorption ( $\Delta G_{\text{vdW}}$ ) is given by

$$\Delta G_{\text{vdW}} = -\frac{A_{132}a}{6h} \quad (3)$$

where  $A_{132}$  is the effective Hamaker constant for the interaction between the flat surface (1) and spherical particle (2) across a medium (3). This may be used to approximate the adsorption of a biomolecule (2) dissolved in an aqueous media (3) to a fluid interface (1). The radius of the sphere is  $a$ , and the distance of closest approach between the sphere surface and the interface is  $h$ . Equation 3 is formulated for the specific case where  $h$  is smaller than  $a$ .

The following combining rule is used to approximate the effective Hamaker constant,  $A_{132}$ , from the individual Hamaker constants ( $A_{ii}$ )

$$A_{132} = (\sqrt{A_{11}} - \sqrt{A_{33}})(\sqrt{A_{22}} - \sqrt{A_{33}}) \quad (4)$$

For a compressible fluid, the individual Hamaker constant can be calculated using Lifshitz theory

$$A_{11} = \frac{3}{4}kT\left(\frac{\epsilon - 1}{\epsilon + 1}\right)^2 + \frac{3h\nu_e}{16\sqrt{2}}\frac{(n^2 - 1)^2}{(n^2 + 1)^{3/2}} \quad (5)$$

where  $k$  is the Boltzmann constant,  $h$  is Planck's constant,  $\nu_e$  is the maximum ultraviolet adsorption frequency ( $3.0 \times 10^{-15}$  s),  $\epsilon$  is the dielectric constant, and  $n$  is the refractive index. For compressed ethane and CO<sub>2</sub>,  $\epsilon$  and  $n$  are functions of density, which were calculated from Lewis et al.<sup>40</sup> Hamaker constant values for propane and N<sub>2</sub> were calculated from Wu et al. ( $A_{11} = \pi^2 C_{11} \rho^2$ , where  $C_{11}$  is a fluid-dependent constant and  $\rho$  is density).<sup>41</sup> The strong dependence of the Hamaker constant on density demonstrates the ability to manipulate the attraction between a colloidal system and a compressible fluid interface by varying the temperature and pressure (Figure 7). Abrupt increases in  $A_{11}$  occur at the vapor–liquid transition. Thus, the rate of adsorption and the apparent equilibrium surface activity of an adsorbing molecule, if dominated by attractive interactions at the water/compressed fluid interface, are expected to be functions of pressure.

The effective Hamaker constants ( $A_{132}$ , eq 4) between lysozyme and the compressed fluid/water interfaces roughly correlate with our observed surface activity measurements (Table 1). For lysozyme,  $A_{132}$  is negative for all compressed fluid interfaces except propane, demonstrating a repulsive protein–interface force ( $\Delta G_{\text{vdW}} > 0$ ) due to dispersion forces (repulsion at 7.0 MPa; N<sub>2</sub> > CO<sub>2</sub> > ethane, Table 1). As  $A_{132}$  increases,

the initial rate of lysozyme adsorption at 7.0 MPa increases, where the rate in propane > ethane > CO<sub>2</sub> > N<sub>2</sub> > air (0.1 MPa) (Figure 2). Furthermore, higher surface pressures are observed in propane with increasing pressure, consistent with an increase in the attractive interaction suggested by the  $A_{132}$  values. The trend with  $A_{132}$  is not observed for increasing CO<sub>2</sub> pressure, where the initial rate and pseudo-equilibrium value of the surface response is greater at 7.0 MPa than at 15.0 MPa despite an increase in density from 16.9 to 19.9 mol/L at 298 K, respectively. This deviation further highlights the unique behavior observed in CO<sub>2</sub>/water systems and the potential role of CO<sub>2</sub>–H<sub>2</sub>O complex organization.

Rapid lysozyme adsorption has been reported at oil/water interfaces owing to attractive dispersion interactions.<sup>3,28</sup> While these interactions appear to play a role in lysozyme adsorption at compressed fluid interfaces, the potential exists for an attractive electrostatic double-layer interaction between lysozyme and the propane, ethane, or CO<sub>2</sub>/water interface. The high rate of initial lysozyme adsorption at the ethane and CO<sub>2</sub> interfaces despite (calculated) repulsive van der Waals interactions (Table 1) may be attributed to electrostatic interactions, such as attractive charge–charge interactions between positively charged lysozyme and anion-bound oil/water interfaces. Further discussion of such interactions on protein adsorption at compressed fluid interfaces requires a better understanding of the binary aqueous/fluid interface.

The pseudo-equilibrium interfacial tension and degree of interfacial repulsion, as determined from  $A_{132}$ , is significantly lower for DPPC at the CO<sub>2</sub>/water interface relative to the air/water interface (Table 2). While the dispersive interaction between DPPC and the compressed CO<sub>2</sub> interface is repulsive, it becomes less repulsive as pressure increases. Similar to lysozyme, the initial DPPC surface response (Figure 6) does not correlate with a reduction in the repulsive interaction as suggested by the effective Hamaker constant. As discussed, the DPPC phase behavior at lower pressures yields a more compressible liquid-expanded monolayer. Therefore, the phase behavior of DPPC appears to play a significant role in the dynamic surface response at the CO<sub>2</sub> interface relative to dispersion forces.

In addition to providing insight into protein precipitation/purification, microbial sterilization, and liposome formation techniques, the dynamic adsorption behavior of enzymes and model cell membranes may help to interpret cell toxicity in developing biphasic aqueous/compressed solvent bioprocesses. For instance, we have demonstrated that high-pressure biphasic incubations lead to phase toxicity (due to the presence of the water/solvent interface), which may be the primary cause of cell inactivation with compressed solvents in both nongrowing<sup>8,9</sup> and growing<sup>41</sup> *Clostridium thermocellum*. The traditional predictor of biocompatibility in the presence of a solvent, the octanol/water partition coefficient ( $\log P$ ), is nearly constant with pressure and solvent phase and is only a weak function of temperature for compressed ethane, propane, CO<sub>2</sub>, and N<sub>2</sub> at the conditions investigated.<sup>8</sup> In our previous work,<sup>43</sup> we observed cell inactivation in the presence of liquid propane and minimal inactivation in the presence of gaseous propane, despite the fact that propane has the same  $\log P$  value in both the gaseous and the liquid state. Therefore,  $\log P$  fails to describe the strong pressure dependence of biocompatibility in thermophilic bacteria in the presence of compressed solvents. In contrast, approaches based on colloidal theory, such as the determination of the effective Hamaker constant, are sensitive to temperature, pressure, phase, and solvent type. This further highlights the



relevance of examining biomolecule interactions at compressed fluid interfaces and interpreting them based on dispersion forces.

## Conclusions

Appreciable surface activity was observed for a model protein (lysozyme) and a model cellular membrane phospholipid (DPPC vesicles) at the interface between an aqueous phase and compressed propane, ethane, CO<sub>2</sub>, and N<sub>2</sub>. The choice of pressurized fluid and the pressure-dependent solvent power of these fluids affects the rate of adsorption, protein conformational changes, or vesicle destabilization as well as the pseudo-equilibrium surface pressure. Unlike compressed N<sub>2</sub> and air, induction periods were not observed at the liquid propane, ethane, and CO<sub>2</sub> interface, denoting rapid adsorption and protein conformational changes. Furthermore, unique surface responses were observed for lysozyme at the CO<sub>2</sub>/water interface. At high CO<sub>2</sub> pressures (15 MPa and 298 K) a lysozyme–CO<sub>2</sub>–H<sub>2</sub>O complex is believed to form in agreement with previous results for ovalbumin.<sup>20</sup> Rapid DPPC vesicle adsorption and destabilization was also observed at the supercritical CO<sub>2</sub> interface (<15 min). High surface pressures in the presence of gaseous CO<sub>2</sub> (1.8 and 3.5 MPa) are consistent with a monolayer of coexisting liquid-condensed and liquid-expanded DPPC domains. In contrast, a liquid-expanded DPPC monolayer was observed at supercritical CO<sub>2</sub> pressures  $\geq$  8.7 MPa. The observed interfacial phase behavior is consistent with our previous work involving CO<sub>2</sub>-induced melting point depression in DPPC bilayers.

Colloidal theory of dispersion forces qualitatively described lysozyme and DPPC interactions at compressed and supercritical fluid interfaces. At 7.0 MPa and 298 K, the rate of lysozyme adsorption correlated with the magnitude of the Hamaker constant: propane > ethane > CO<sub>2</sub> > N<sub>2</sub> > air (0.1 MPa). The strong density dependence of this attractive force can be used as a “probe” for investigating interfacial properties of biomolecules at a single compressible fluid interface (i.e., attractive vdW interactions can be manipulated with pressure while maintaining constant electrostatic interactions). Although the influence of electrostatic interactions in lysozyme adsorption at propane, ethane, and CO<sub>2</sub> could not be determined explicitly, we have identified potential effects such as interfacial anion binding. Future studies are aimed at investigating the impact of surface-active biomolecules in compressed and supercritical processes such as enzyme catalysis, liposome formation, and microbial metabolism or sterilization.

**Acknowledgment.** The authors gratefully acknowledge the financial support of the National Science Foundation (BES-9817069), the NSF Research Experience for Undergraduates program (DMR-0097692), and the NSF Discovery Corps Fellowship program (CHE-0412109).

## References and Notes

- (1) Bar, R. *J. Chem. Technol. Biotechnol.* **1988**, *43*, 49.

- (2) Osborne, S. J.; Leaver, J.; Turner, M. K.; Dunnill, P. *Enzymol. Microb. Technol.* **1990**, *12*, 281.
- (3) Beverung, C. J.; Radke, C. J.; Blanch, H. W. *Biophys. Chem.* **1999**, *81*, 59.
- (4) Heurtault, B.; Saulnier, P.; Pech, B.; Proust, J.-E.; Benoit, J.-P. *Biomaterials* **2003**, *24*, 4283.
- (5) Pautot, S.; Frisken, B. J.; Weitz, D. A. *Langmuir* **2003**, *19*, 2870.
- (6) Jarzebski, A. B.; Malinowski, J. J. *Process Biochem.* **1995**, *30*, 343.
- (7) Randolph, T. W. *TIBTECH* **1990**, *8*, 78.
- (8) Berberich, J. A.; Knutson, B. L.; Strobel, H. J.; Tarhan, S.; Nokes, S. E.; Dawson, K. A. *Biotechnol. Bioeng.* **2000**, *70*, 491.
- (9) Berberich, J. A.; Knutson, B. L.; Strobel, H. J.; Tarhan, S.; Nokes, S. E.; Dawson, K. A. *Ind. Eng. Chem. Res.* **2000**, *39*, 4500.
- (10) Knez, Z.; Habulin, M. *J. Supercrit. Fluids* **2002**, *23*, 29.
- (11) Mesiano, A. R.; Beckman, E. J.; Russell, A. J. *Chem. Rev.* **1999**, *99*, 623.
- (12) Randolph, T. W.; Blanch, H. W.; Prausnitz, J. M. *Biotechnol. Lett.* **1985**, *7*, 325.
- (13) Ghenciu, E. G.; Beckman, E. J. *Ind. Eng. Chem. Res.* **1997**, *36*, 5366.
- (14) Jung, J.; Perrut, M. *J. Supercrit. Fluids* **2001**, *20*, 179.
- (15) Frederiksen, L.; Anton, K.; van Hoogevest, P.; Keller, H. R.; Leuenberger, H. J. *J. Pharm. Sci.* **1997**, *86*, 921.
- (16) Otake, K.; Imura, T.; Sakai, H.; Abe, M. *Langmuir* **2001**, *17*, 3898.
- (17) Spilimbergo, S.; Elvassore, N.; Bertucco, A. *J. Supercrit. Fluids* **2002**, *22*, 55.
- (18) Dillow, A. K.; Dehghani, F.; Hrkach, J. S.; Foster, N. R.; Langer, R. *Proc. Natl. Acad. Sci. U.S.A.* **1999**, *96*, 10344.
- (19) Shah, P. S.; Hanrath, T.; Johnston, K. P.; Korgel, B. A. *J. Phys. Chem. B* **2004**, *108*, 9574.
- (20) Tewes, P.; Boury, F. *J. Phys. Chem. B* **2005**, *109*, 1874.
- (21) Bothun, G. D.; Knutson, B. L.; Strobel, H. J.; Nokes, S. E. *Langmuir* **2005**, *21*, 530.
- (22) Ambwani, D. S.; Fort, J., T. Pendant Drop Technique for Measuring Liquid Boundary Tensions. In *Surface and Colloid Science*; Plenum Press: New York, 1979; Vol. 11, p 93.
- (23) Stauffer, C. E. *J. Phys. Chem.* **1965**, *69*, 1933.
- (24) Wiegand, G.; Franck, E. U. *Ber. Bunsen-Ges. Phys. Chem.* **1994**, *98*, 809.
- (25) Tripp, B. C.; Magda, J. J.; Andrade, J. D. *J. Colloid Interface Sci.* **1995**, *173*, 16.
- (26) Miller, R.; Fainerman, V. B.; Makievski, A. V.; Kragel, J.; Grigoriev, D. O.; Kazakov, V. N.; Sinyachenko, O. V. *Adv. Colloid Interface Sci.* **2000**, *86*, 39.
- (27) Ninham, B. W.; Kurihara, K.; Vinogradova, O. I. *Colloids Surf., A* **1997**, *123*, 7.
- (28) Sengupta, T.; Damodaran, S. *Langmuir* **1998**, *14*, 6457.
- (29) DeSimone, J.; Guan, Z.; Elsbernd, C. *Science* **1992**, *257*, 945.
- (30) Kazarian, S. G.; Vincent, M. F.; Bright, F. V.; Liotta, C. L.; Eckert, C. A. *J. Am. Chem. Soc.* **1996**, *118*, 1729.
- (31) Tewes, P.; Boury, F. *J. Phys. Chem. B* **2004**, *108*, 2405.
- (32) Chun, B.-S.; Wilkinson, G. T. *Ind. Eng. Chem. Res.* **1995**, *34*, 4371.
- (33) Hebach, A.; Oberhof, A.; Dahmen, N.; Kogel, A.; Ederer, H.; Dinjus, E. *J. Chem. Eng. Data* **2002**, *47*, 1540.
- (34) Gugliotti, M.; Politi, M. *J. Biophys. Chem.* **2001**, *89*, 243.
- (35) Panaiotov, I.; Ivanova, T.; Balashev, K.; Proust, J. *Colloids Surf., A* **1995**, *102*, 159.
- (36) Koynova, R.; Caffrey, M. *Chem. Phys. Lipids* **2002**, *115*, 107.
- (37) Li, J. B.; Miller, R.; Mohwald, H. *Colloids Surf., A* **1996**, *114*, 123.
- (38) Yang, B.; Matsumura, H.; Furusawa, K. *Colloids Surf., B* **1999**, *14*, 161.
- (39) Israelachvili, J. N. *Intermolecular and Surface Forces*; Academic Press: London, U. K., 1992.
- (40) Lewis, J. E.; Biswas, R.; Robinson, G.; Maroncelli, M. *J. Phys. Chem. B* **2001**, *105*, 3306.
- (41) Wu, J.; Prausnitz, J. M.; Firoozabadi, A. *AIChE J.* **2000**, *46*, 197.
- (42) Israelachvili, J. N. *Langmuir* **1994**, *10*, 3369.
- (43) Bothun, G. D.; Knutson, B. L.; Strobel, H. J.; Nokes, S. E. *Biotechnol. Bioeng.* **2004**, *89*, 32.